Fault-Tolerant Control for Automated Highway Systems

Jeffrey T. Spooner and Kevin M. Passino, *Senior Member, IEEE*

***Abstract*— Increasing highway traffic congestion and real estate costs that limit the building of new highways has brought about a renewed interest in an Automated Highway System (AHS) where the vehicle steering task ("lateral control") and the braking/throttle tasks ("longitudinal control") are taken over by computers to increase the throughput of existing highways. Since safety plays a key role in the development of an AHS, fault-tolerant control is vital. In this paper, we develop a robust longitudinal sliding-mode control algorithm and prove that this control algorithm is stable for a certain class of faults. In addition, we show that intervehicle spacing errors will not become amplified along the AHS in the event of a loss of lead vehicle information. The performance of the sliding-mode controller is demonstrated through a series of simulations incorporating various vehicle and AHS faults.**

***Index Terms*— Automated highway systems, automatic vehicle control systems, fault tolerance, lateral vehicle control, longitudinal vehicle control, sliding-mode control.**

I. Introduction

THE CONCEPT of an Intelligent Transportation System (ITS) has been developed out of the need for increased highway efficiency and car carrying capacity while improving safety and ease of travel at a low cost [1]. The Automated Highway System (AHS) is a key component in the movement toward an advanced ITS for vehicles on highways. Upon entering the AHS, on-board lateral and longitudinal control systems will drive an automobile along the fully automated highway. To enable this, each automobile will be equipped with control systems which coordinate control between the brakes, engine, and steering subsystems. The longitudinal control system is responsible for maintaining vehicle speed and a safe "headway" to the vehicle it is following, while the lateral controller is responsible for tracking a desired trajectory along the highway. With fully automated driving, the car carrying capacity of current highways may be greatly increased, while actually increasing the highway safety due to a reduction in human error. To further increase the efficiency and safety of the highway systems, additional supervisory systems, such as an Advanced Traffic Management Systems (ATMS), may be used to schedule efficient routes, taking into account current weather conditions, highway incidents, and congestion [2]. See [1]–[4] for an overview of the ITS effort.

Different traffic configurations have been considered with regard to the intervehicle spacing within an AHS. The predominant approaches are platooning and uniform spacing headway policies. Under platooning, the vehicles are grouped together such that the intervehicle spacing within the platoon is very small (e.g., 1 m), while the spacing between platoons is rather large (e.g., 100 m). If a highway incident occurs such that the lead vehicle in the platoon applies emergency braking, none of the vehicles within the platoon will collide with one another with a large relative velocity due to the small intervehicle spacing [2]. The uniform spacing headway policy takes a slightly different view, in that the there is a moderate intervehicle spacing (e.g., 20 m), so that collisions are avoided during emergency braking situations. Platooning may double the traffic flow rates obtained using a uniform headway policy, however, safety and human factors must be taken into consideration. Within the different traffic configurations, the intervehicle spacing may be constant or velocity-dependent. Within this paper, a velocity-dependent headway policy is used where the parameters may be set so that either platooning or a uniform headway policy may be implemented.

In [5], it was shown that feedback linearization techniques may be used to achieve stable operation of a platoon of vehicles with constant intervehicle spacing if information about the lead vehicle was available to each following vehicle, while later in [6] the effects of communication losses between vehicles were considered. The controller proposed herein allows for the incorporation of lead vehicle information, however, we show that it is not required to provide a safe driving environment. Our controller development allows for varying degrees of vehicle intelligence so that a combination of manual and AHS-equipped vehicles may share the same automated lane. This approach may aid in the initial AHS development when a dedicated automated lane may not be available.

Using a velocity-dependent intervehicle spacing law, it was shown in [7] that intervehicle spacing oscillations may be eliminated if vehicle parameters are known so that nonlinearities within the vehicle dynamics may be canceled. This "constant-time headway policy" was then used within [8] to provide a stable entrainment policy. It was shown in [9] that variable structure techniques may be used for stable longitudinal control if lead vehicle information is available to each following vehicle, and was later shown in [10] that using a constant time

Manuscript received May 19, 1995; revised December 21, 1995. This work was supported by the CITR at Ohio State University and the National Science Foundation under Grants IRI-9210332 and EEC-9315257. The work of J. T. Spooner was supported by a Fellowship from the Center for Intelligent Transportation Research (CITR) at Ohio State University.

J. T. Spooner was with the Department of Electrical Engineering, Ohio State University, Columbus, OH 43210 USA. He is now with Sandia National Laboratories, Albuquerque, NM, 87185-0503 USA (e-mail: jtspoon@sandia.gov).

K. Passino is with the Department of Electrical Engineering, Ohio State University, Columbus, OH 43210 USA (e-mail: passino@ee.eng.ohio-state.edu).

Publisher Item Identifier S 0018-9545(97)04640-9.

headway policy, platoon stability may be achieved. Within this paper, we use a constant time headway policy and a different variable structure control formulation due to a more complex automobile model containing independent engine and brake dynamics.

Though a great deal of research effort has been invested to solve AHS related problems, relatively little has been done to address issues of fault tolerance. Within this paper, issues of control system tolerance of automobile and AHS faults are addressed in conjunction with the controller designs, and a collision avoidance scheme is introduced to improve the safety of the AHS. The collision avoidance scheme is used to ensure that if a vehicle tracks its assigned position within a string, then it will not follow the preceding vehicle at an unsafe distance. Varying degrees of fault severity may occur, including minor faults such as tire misalignment and brake inefficiency due to overheating, up to major faults such as complete engine failure. Here we use techniques from robust control to address relatively minor faults so that it is still possible to drive the automobile with degraded performance.

This paper is organized as follows: In Section II, a simplified model (relative to the one in [11] that we use in our simulations as a "truth" model) of an automobile is derived, including the longitudinal, engine and brake dynamics. In Section III, the class of automobile faults are defined for which our control system will be robust. Section IV defines the sliding-mode system and proves local stability of the controller. Section V demonstrates the controller performance in the presence of various automobile and AHS faults through a series of simulations, while concluding remarks are presented within Section VI.

II. Automobile and Automated Lane Model

To develop a fault-tolerant controller for use in an automated lane, a model which takes into account the principle automobile dynamics, while remaining simple enough for control design, is necessary.

A. Automobile Dynamics

In our model, which is based on the one in [11], g is the gravitational acceleration, m is the total automobile mass, and I_x, I_y, and I_z are the moments of inertia for the total automobile mass about the x, y, and z axes, respectively. The automobile angular velocities ω_x, ω_y, and ω_z are defined about the x, y, and z axes, respectively. The distances a, b, c, and d are defined from the automobile center of gravity as depicted in Fig. 1. A_{ρ_x} and A_{ρ_y} are the coefficients of aerodynamic drag in the x and y directions, respectively, with v_{air_x} and v_{air_y} the ground velocity of the air in the body fixed reference frame along the x and y directions, respectively. The forces on the nth tire are separated into a circumferential force C_n and a lateral force L_n, with δ_n the angle between the nth tire's circumferential direction and the direction of travel of the automobile center of gravity. The tire forces in the x and y directions on the nth wheel are F_{x_n} and F_{y_n}, respectively. The road angles $\hat{\theta}_r$ and $\hat{\phi}_r$ are defined about the x and y axes, respectively. The equations of motion for the automobile's total mass center are defined as

$$m(\ddot{x} - \dot{y}\omega_z + \dot{z}\omega_y) = \sum_{n=1}^{4} F_{x_n} + mg \sin \hat{\theta}_r - A_{\rho_x}(\dot{x} - v_{air_x})^2 \tag{1}$$

$$m(\ddot{y} + \dot{x}\omega_z - \dot{z}\omega_x) = \sum_{n=1}^{4} F_{y_n} - mg \sin \hat{\phi}_r \cos \hat{\theta}_r - A_{\rho_y}(\dot{y} - v_{air_y})^2 \tag{2}$$

$$I_z\dot{\omega}_z - (I_x - I_y)\omega_x\omega_y = a(F_{y_1} + F_{y_2}) - b(F_{y_3} + F_{y_4}) - c(F_{x_1} + F_{x_4}) + d(F_{x_2} + F_{x_3}) \tag{3}$$

where

$$F_{x_n} = C_n \cos \delta_n - L_n \sin \delta_n$$
$$F_{y_n} = C_n \sin \delta_n + L_n \cos \delta_n. \tag{4}$$

When developing a model for controller design, it is desirable to distinguish between measurable and unmeasurable terms. Within this development, it is assumed that quantities such as ground air speeds and road angles are not measurable, and although gyroscopes may be used, it is also assumed that the angular velocities, ω_x and ω_y, cannot be measured (later we show that only states $\dot{x}$ and $\ddot{x}$, possibly along with engine and brake states, need to be measured in conjunction with AHS measurements for control). Since current automobiles in general do not allow for rear wheel steering, and the front wheels move together, we assign $\delta := \delta_1 = \delta_2$ (see Fig. 1 for wheel numbering) and $\delta_3 = \delta_4 = 0$. A further assumption is made so that the turning of the automobile is due to the steering angle of the wheels, and not differential tractive forces between the tires, so that $cF_{x_1} = dF_{x_2}$ and $cF_{x_4} = dF_{x_3}$. To simplify notation, consider the front tire circumferential forces $C_f := C_1 + C_2$, the rear tire circumferential forces $C_r := C_3 + C_4$, and the front tire lateral forces $L_f := L_1 + L_2$. We may now express (1) as

$$m(\ddot{x} - \dot{y}\omega_z) = C_f \cos \delta + C_r - L_f \sin \delta + mg \sin \hat{\theta}_r - A_{\rho_x}(\dot{x} - v_{air_x})^2 - m\dot{z}\omega_y. \tag{5}$$

Now, we use a small-angle approximation for functions containing δ, and group unmeasurable terms together as disturbances, so that

$$m(\ddot{x} - \dot{y}\omega_z) = C_f + C_r - L_f\delta - A_\rho\dot{x}^2 + d_{x1} \tag{6}$$

where

$$d_{x1} = -m\dot{z}\omega_y + C_f(\cos \delta - 1) - L_f(\sin \delta - \delta) + mg \sin \hat{\theta}_r - A_{\rho_x}(v_{air_x}^2 - 2\dot{x}v_{air_x}). \tag{7}$$

As is standard, we will call d_{x1} a disturbance since it represents dynamics of the plant that are not explicitly used in the development of the control algorithm (it could represent deterministic, but unknown, influences rather than stochastic ones).

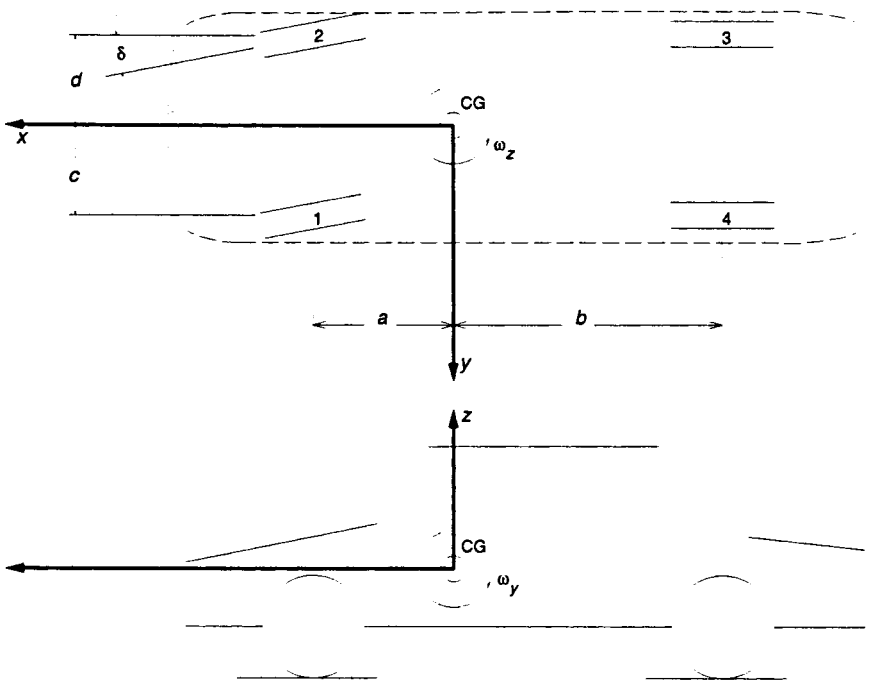

Fig. 1. Automobile dimensions and numbering for modeling.

B. Power Train and Brakes

The driving force is applied as a torque from the engine, which then passes through the torque converter and the transmission and differential gears to the rear wheels.[1] The torque on the wheels is then converted to a driving force through the interaction between the road and tires. Assume that the angular velocity of the left and right front tires (ω_{a_1} and ω_{a_2}) are equal and the angular velocity of the left and right rear tires (ω_{a_3} and ω_{a_4}) are equal, so that $\omega_{a_f} := \omega_{a_1} = \omega_{a_2}$ and $\omega_{a_r} := \omega_{a_3} = \omega_{a_4}$. The driving force in the circumferential direction of the rear tires is defined by

$$C_{d_r} := \frac{1}{RR_g}\, h_d(\dot{x}, \omega_{a_r}, F_r, \omega_e)T_e \tag{8}$$

where T_e is the engine torque applied to the torque converter, R is the tire radius, and R_g is the gear reduction due to the transmission and differential. The driving torque transfer factor $h_d(\cdot)$ takes into account the possible reduction in torque transfer due to the wheel slip and/or the possible amplification in torque due to the torque converter. The driving torque transfer factor is dependent upon the automobile longitudinal velocity, angular velocity of the wheel axles, the normal forces at the front and rear tires, F_f and F_r, respectively, the engine speed ω_e, and the road/tire characteristics. Since it is not possible to measure $h_d(\cdot)$, we consider $h_d(\cdot)$ to be in the given range

$$h_{dr} := h_d(\dot{x}, \omega_{a_r}, F_r, \omega_e) \in [h_{d_{\min}}, h_{d_{\max}}] \tag{9}$$

with the time derivative $|\dot{h}_{dr}| \leq H_d$, where H_d is a known bound on the derivative.

[1] We consider rear-wheel-drive vehicles so that disturbances due to a combined effect from steering and the throttle are not considered. Overall, however, a methodology similar to the one developed here can be used for front-wheel-drive vehicles.

The braking force is applied to the automobile body through the interaction of the tires and road, however, unlike the driving force, it is not influenced by the drivetrain. The braking forces applied to the front C_{b_f} and rear, C_{b_r} tires in the circumferential direction are given as

$$C_{b_f} = \frac{1}{R}\, h_b(\dot{x}, \omega_{a_f}, F_f)T_{b_f} \tag{10}$$

$$C_{b_r} = \frac{1}{R}\, h_b(\dot{x}, \omega_{a_r}, F_r)T_{b_r} \tag{11}$$

where T_{b_f} and T_{b_r} are the braking torques applied to the front and rear tires, respectively. Since the attenuation in torque from the brake pads to automobile body relies on the interaction between the tires and road, it is assumed that $h_b(\cdot)$ cannot be directly measured. The braking torques are distributed between the front and rear tires according to the brake proportioning factor $f_{bp} \in [0, 1]$, so that

$$T_{b_f} = f_{bp}T_b \tag{12}$$

$$T_{b_r} = (1 - f_{bp})T_b \tag{13}$$

where T_b is the total applied brake force (i.e., $T_b := T_{b_f} + T_{b_r}$). The total braking force may be expressed as

$$C_b = C_{b_f} + C_{b_r} = \frac{1}{R}\, h_{br}T_b. \tag{14}$$

Here

$$h_{br} := h_b(\dot{x}, \omega_{a_f}, F_f)f_{bp} + h_b(\dot{x}, \omega_{a_r}, F_r)(1 - f_{bp}) \in [h_{b_{\min}}, h_{b_{\max}}]$$

(where $h_{b_{\min}}$ and $h_{b_{\max}}$ are known) and the magnitude of the time derivative is bounded by $|\dot{h}_{br}| \leq H_b$, where H_b is a known bound on the derivative.

The induced engine torque T_e is governed by

$$\dot{T}_e = \frac{1}{\tau_e}(-T_e + u_d) + \frac{d_e}{\tau_e} \tag{15}$$

where $\tau_e > 0$ is due to the engine time constant and throttle actuator delay, $u_d \geq 0$ is the commanded engine (or driving) torque, and $d_e \leq D_e(X, t)$ (X will be defined below) is the engine disturbance whose magnitude is bounded above by the known function $D_e(X, t)$. The engine disturbance may occur, for example, due to the auxiliary (load) torque of an air conditioner. A simple model of an engine was used here so that a wide range of engine types and models could be approximated using an appropriate torque map. Although internal combustion engines are used almost exclusively at this time, in the future electric engines may become more common. Within this paper, the torque map is defined to approximate the four-stroke fuel-injected engine described in [12]. The commanded engine torque is given as

$$u_d = T_{\max} \frac{\dot{m}_{ao}}{\omega_e} \text{AFI} \tag{16}$$

where $T_{\max}$ is related to the engine torque capacity, $\dot{m}_{ao}$ is the mass flow rate of the air leaving the intake manifold, ω_e is the engine speed, and AFI is the air-to-fuel ratio influence. Here it is assumed that during normal highway driving conditions, the engine speed will always be greater than zero. Since the intake manifold dynamics are typically much faster than the engine's mechanical dynamics, the mass flow rate exiting the manifold may be expressed as a mapping from the throttle angle $\alpha \geq 0$

$$\dot{m}_{ao} = \text{MAX} \cdot \text{TC}(\alpha). \tag{17}$$

MAX is the maximum mass flow rate, and the normalized throttle characteristic TC is given as [12]

$$\text{TC}(\alpha) = \begin{cases} 1 - \cos\left[(1.144\,59\alpha - 1.0600)\dfrac{\pi}{180}\right], & \alpha \leq 79.46 \\ 1, & \alpha > 79.46. \end{cases} \tag{18}$$

The brake torque dynamics are similarly modeled as a first order lag

$$\dot{T}_b = \frac{1}{\tau_b}(-T_b + u_b) + \frac{d_b}{\tau_b} \tag{19}$$

where $\tau_b > 0$ is the time constant for the brakes and brake actuator $u_b \in [-T_{b_{\max}}, 0]$ is the commanded brake torque, and $d_b \leq D_b(X, t)$ is a brake torque disturbance bounded by the known function $D_b(X, t)$. The automobile longitudinal dynamics state vector is given as $X := [x\ \dot{x}\ T_e\ T_b]^T$. The vehicle dynamics will now be converted to a normal form more suited for control development.

Using (6), the longitudinal dynamics may be expressed as

$$\ddot{x} = \frac{1}{m}\left[\frac{1}{RR_g} h_{dr} T_e + \frac{1}{R} h_{br} T_b - A_{\rho_x}\dot{x}^2\right] + d_{x2}(X, t) \tag{20}$$

where the new longitudinal disturbance is given by

$$d_{x2}(X, t) := \frac{d_{x1}(X, t)}{m} - \frac{2\hat{C}\delta}{m}\left(\delta - \frac{\dot{y} + a\omega_z}{\dot{x}}\right) + \frac{\dot{x}\dot{y}}{\rho} \tag{21}$$

where d_{x1} is defined in (7). In the development to follow, the time derivative of the longitudinal acceleration is needed, so using (15) and (19), we obtain

$$\begin{aligned} x^{(3)} = \frac{1}{m}\Bigg[&\frac{1}{RR_g\tau_e} h_{dr}(-T_e + u_d + d_e) \\ &+ \frac{1}{R\tau_b} h_{br}(-T_b + u_b + d_b) - 2A_{\rho_x}\dot{x}\ddot{x}\Bigg] \\ &+ d_{x3}(X, t) \end{aligned} \tag{22}$$

where $x^{(i)}$ denotes the ith derivative of x and

$$d_{x3}(X, t) = \frac{1}{mRR_g}\dot{h}_{dr} T_e + \frac{1}{mR}\dot{h}_{br} T_b + \dot{d}_{x2}(X, t). \tag{23}$$

This disturbance may be bounded by

$$\begin{aligned} |d_{x3}(X, t)| &\leq D_{x3}(X, t) \\ &:= \frac{1}{mRR_g} H_d T_e - \frac{1}{mR} H_b T_b + |\dot{d}_{x2}(X, t)| \end{aligned} \tag{24}$$

(recall that $T_e \geq 0$ and $T_b \leq 0$). Notice by the definition of $d_{x3}(X, t)$, that the size of the disturbances depends upon the road, atmospheric conditions (e.g., wind), and the dynamics of the automobile itself.

III. Automobile and AHS Faults

This study is primarily concerned with robust control of automobiles within an automated lane for four separate classes of faults. These faults are 1) reduction in effective braking; 2) reduction in the effective power transfer between the engine and the automobile longitudinal dynamics; and 3) the loss of accurate sensor information used to guide the automobiles along an automated highway. The faults associated with braking and driving may be initiated by either the associated actuators or some failure in the physical system itself. Faults associated with the automated lane, however, are typically due to sensor failures used to determine intervehicular spacing. Within this paper, only faults which still allow the automobile to be driven within the automated lane will be considered (then, e.g., *complete* failure of the brake or engine subsystems is not considered).

In this paper, we will focus on faults which enter as an additive term to the disturbance $d_{x3}(X, t)$, and/or as a multiplicative term to the torque gains. To do this, we modify the longitudinal dynamics in (22) to

$$\begin{aligned} x^{(3)} = \frac{1}{m}\Bigg[&\frac{1}{RR_g\tau_e} h_{dr}(-T_e + \gamma_d u_d + d_e) \\ &+ \frac{1}{R\tau_b} h_{br}(-T_b + \gamma_b u_b + d_b) - 2A_{\rho_x}\dot{x}\ddot{x}\Bigg] \\ &+ \frac{d}{dt}\Delta f_x + d_{x3}(X, t) \end{aligned} \tag{25}$$

where γ_d is a multiplicative term that can be used to represent a reduction in engine power, γ_b represents reductions in the braking torque, and $m\Delta f_x$ are added longitudinal forces due to faults. With no faults, (25) reduces to (22) with $(d/dt)\Delta f_x = 0$ and $\gamma_d = \gamma_b = 1$. To reject the effects of the faults, it is necessary to know the bounds on the faults, that is, we assume $0 \leq |(d/dt)\Delta f_x| \leq F_x$ (for some $F_x > 0$),

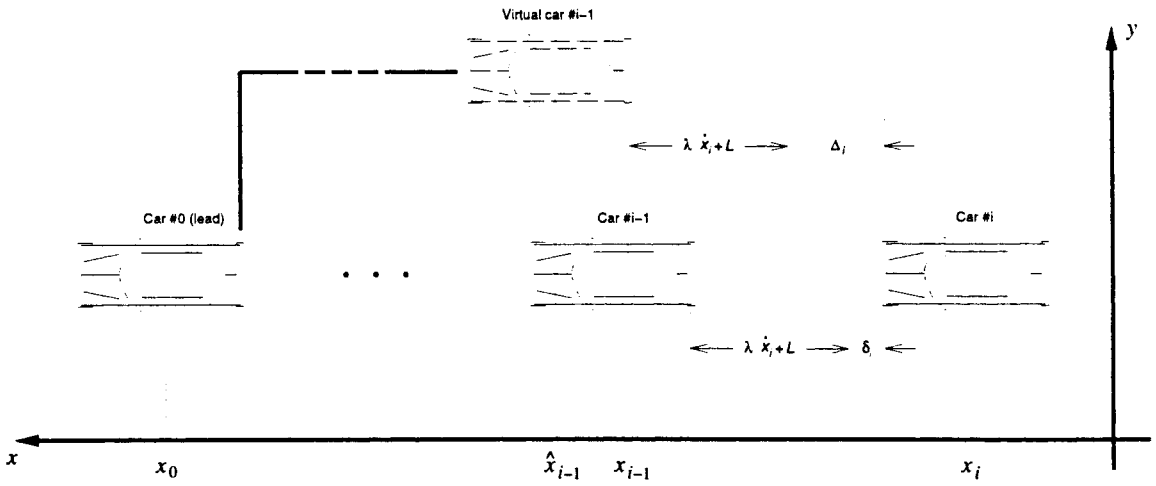

Fig. 2. Car following within an Automated Highway System.

$\gamma_d \in [\gamma_{d_{\min}}, \gamma_{d_{\max}}]$, and $\gamma_b \in [\gamma_{b_{\min}}, \gamma_{b_{\max}}]$ where $\gamma_{d_{\min}} > 0$ and $\gamma_{b_{\min}} > 0$. Even though the bounds on the faults are needed (and in practice obtainable), the specific time-varying behavior of the faults is not needed.

Faults within the AHS may result from the loss of sensor information, or from sensor errors, including gains, offsets, or noise in measurements. For example, a sensor may indicate that the spacing between the ith and $i-1$st vehicle is 10 m, when in reality there is only 5 m between them. Sensor redundancy may be used to check the validity of each measurement, however, here we will simply assume that each measurement is correct for controller development, and through simulations demonstrate how the AHS faults affect the overall performance of the system. If the communication signal is lost between automobiles so that the ith automobile has no information about vehicles in front of the $i-1$st vehicle, then we need to ensure that the AHS safety is not reduced to a point at which collisions might occur.

IV. Controller Development

Since the lateral velocity of an automobile traveling along a highway is very small with respect to the longitudinal velocity, the relative velocity between the ith and $i-1$st vehicles may be expressed as

$$\dot{\Psi}_i \approx \dot{x}_i - \dot{x}_{i-1}. \tag{26}$$

This implies that for controller development, the distance between the center of gravity of the ith and $i-1$st automobiles may be expressed as $\Psi_i = x_i - x_{i-1}$.

A. The AHS Headway Policy

Within an AHS it may be possible to have varying degrees of "intelligence" among the vehicles. For example, there may be "dumb" vehicles which have no AHS capabilities, vehicles equipped with a radar to determine longitudinal and lateral spacing information, and vehicles which have both a radar system and a communication link with the vehicle it is following within the AHS. Here, the communication link may be used to transmit cumulative position and velocity error along a string of following vehicles. Allowing for a wide range of vehicle intelligence will allow for an easier transition from current highways to AHS since AHS lanes will not need to be separate from conventional non-AHS lanes.

It is desirable to be able to increase the spacing between automobiles as the vehicle speed increases so that the automobiles may safely stop in case of an emergency. For our study, we will seek to maintain a distance of $\lambda_i \dot{x}_i + L_i$ between vehicles i and $i-1$ (see Fig. 2). We will assume that $\lambda_i = \lambda$ and $L_i = L$ for all i. Although one could also add a dependency on vehicle acceleration or other variables, this velocity-dependent "headway policy" (also known as a constant-time headway policy) is consistent with modern driving rules, such as allowing one car length between you and the car in front of you for each 10 mi/h. For example, if you are traveling at 60 mi/h, spacing of at least six car lengths should be maintained. The spacing error between the ith and $i-1$st cars is defined as[2]

$$\delta_i := \Psi_i + \lambda \dot{x}_i + L + M_i \tag{27}$$

$$= x_i + \lambda \dot{x}_i + L + M_i - x_{i-1}. \tag{28}$$

The actual distance between the automobiles is given by $\Phi_i := x_{i-1} - M_i - x_i$, where $M_i > 0$ is the distance between the ith and $i-1$st automobile centers of gravity if the front of the ith automobile just is touching the rear of the $i-1$st automobile (recall that the positive x direction is from the following vehicles, toward the lead vehicle). Thus δ_i is the spacing error, defined by the difference between the desired intervehicle spacing and the actual intervehicular spacing between the ith and $i-1$st vehicles. The one vehicle length per 10-mi/h rule, with a vehicle length of 4 m, corresponds roughly to $\lambda = 0.9$ and $L = 0$ (for this example, if each vehicle is identical, $M_i = 4$). This value represents safe human driving, though headway policies for an AHS may use much smaller values of λ, thus increasing the highway carrying capacity.

[2] Please note that we use δ_i here as the spacing error and earlier as the wheel angle; however, note that for the wheel angles we assumed rear-wheel drive and made the two front steered wheels move together so that our steering angle is δ (with no subscript) so that there is no confusion between the two variables.

Thus far we have defined the intervehicle spacing error δ_i between individual vehicles. Now we consider a spacing error between the ith and lead vehicles. The "cumulative spacing error" for the ith vehicle is

$$\sum_{k=1}^{i} \delta_k = x_i + iL + \sum_{k=1}^{i} (\lambda \dot{x}_i + M_i) - x_0 \tag{29}$$

where the vehicles are numbered such that $i = 0$ corresponds to the lead vehicle, $i = 1$ corresponds to the first following vehicle, and so on. If a controller is designed to ensure that the cumulative error for each vehicle is driven to zero, it is possible that disturbances acting upon the jth vehicle, where $0 < j < i$, will cause the ith vehicle to also feel the effects of the disturbance. This occurs largely due to the velocity dependence upon the headway policy. If we were to allow $\lambda = 0$, then a standard cumulative error may be used [13]; however, we would lose the low-pass filtering characteristics (discussed in more detail below) of a velocity-dependent headway policy.

Define $\hat{x}_i$ to be the desired global position of the ith vehicle based on the current lead vehicle position and velocity (see Fig. 2), and define the "virtual intervehicle spacing" error for the ith vehicle as

$$\Delta_i := x_i + \lambda \dot{x}_i + L + M_i - \hat{x}_{i-1}. \tag{30}$$

Consider for a moment $L = M_i = 0$, for all $i = 1, \cdots, q$, where there are q following vehicles within a string of vehicles with communication. The virtual positions may be found by setting $\delta_i = 0, i = 1, \cdots, q$, so that $x_{i-1} + \lambda \dot{x}_{i-1} = x_{i-2}$. Setting $\hat{x}_{i-1} + \lambda \dot{\hat{x}}_{i-1} = \hat{x}_{i-2}$ and $\hat{x}_0 = x_0$, then through recursion down the string of vehicles, we obtain

$$\hat{X}_i(s) = \frac{1}{(\lambda s + 1)^i} X_0(s) \tag{31}$$

(where $X_i(s)$ is the Laplace transform of x_i). Unfortunately, we can only measure relative distances with a longitudinal sensor (within this study, we do not consider the use of Global Positioning Systems). Taking the Laplace transform of (30), after some manipulations we obtain

$$X_i(s) - \hat{X}_{i-1}(s) = \frac{(\lambda s + 1)^{i-1} - 1}{s(\lambda s + 1)^{i-1}} s Z_1(s) - \frac{1}{(\lambda s + 1)^{i-1}} Z_2(s) \tag{32}$$

where $z_1(t) = x_i(t)$ and $z_2(t) = x_0(t) - x_i(t)$. Since this is a linear system, we no longer restrict $L = M_i = 0$, so we assign

$$z_2(t) = -L - M_i + \sum_{k=1}^{i} (-\Phi_k + L)$$

where $\Phi_i = x_{i-1} - x_i - M_i$ is the intervehicle spacing between the ith and $i-1$st vehicles obtained using a radar system. If the system is at steady-state (setting $s = 0$), then

$$\Delta_i = \sum_{k=1}^{i} \delta_k$$

is a cumulative spacing error. We notice that the virtual position allows for a filtering of the actual intervehicle spacing errors. This form of the filter was obtained directly by the definition of the headway policy, then setting each intervehicle spacing error δ_i to zero. The constant-time headway policy causes the interaction between each vehicle to ideally behave as a first-order low-pass filter. It is interesting to note that if acceleration were incorporated into the headway policy, the parameters could have been picked such that the interaction between the vehicle would ideally behave as a second-order low-pass filter.

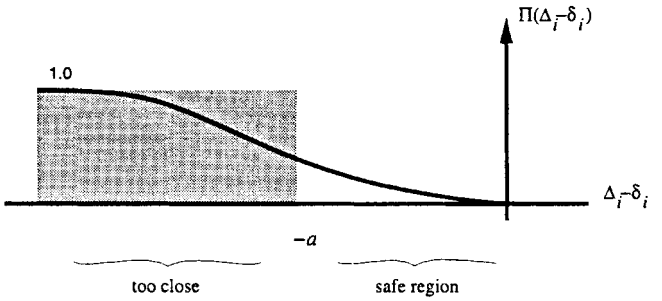

Fig. 3. A choice of $\Pi(\cdot)$ for the collision-avoidance scheme.

B. Collision Avoidance

We wish to develop a longitudinal control law which will guarantee that 1) every following vehicle will maintain a safe distance from the vehicle it is following and 2) if safe intervehicle spacing is maintained, then each following vehicle will be positioned such that the string spacing error Δ_i is minimized. These considerations take both local and global information into account. Global considerations are in terms of the overall string objectives, while local considerations are in terms of an individual vehicle.

If only string spacing error (distance to the lead vehicle) information is available, then the controller for the ith vehicle $(i \geq 2)$ does not know how far away the $i-1$st vehicle is, thus providing a very unsafe driving environment. If the longitudinal controller for the ith vehicle only knows the intervehicle spacing error δ_i then it is possible to avoid collisions and thus provide a safe driving environment, however, "slinky effects" may be introduced into the automated lane. Slinky effects are spacing oscillations which propagate along a string of following vehicles, causing the entire string to constantly grow and contract [7]. This type of behavior may result in a very unpleasant ride for the passengers of the vehicles at the end of the string. If the length of a string of vehicles is allowed to oscillate over a fairly wide range, it may also become particularly difficult for an Advanced Traffic Management System (ATMS) to schedule efficient traffic patterns, thus reducing the effectiveness of the AHS.

A new position error measurement e_i is now defined to take into account the local and global considerations associated with a collision-avoidance scheme

$$e_i = \Delta_i + z_i \tag{33}$$

where

$$z_i = (\delta_i - a - \Delta_i)\Pi(\Delta_i - \delta_i) \tag{34}$$

and $\Pi(\cdot) \in [0, 1]$ is a weighting function (see Fig. 3) defined such that z_i is continuous. The weighting function $\Pi(\cdot)$ is used to take into account the importance of δ_i and Δ_i at any given time. A value of $\Pi(\cdot) = 0$ implies that the following vehicle is a safe distance from the preceding vehicle so that

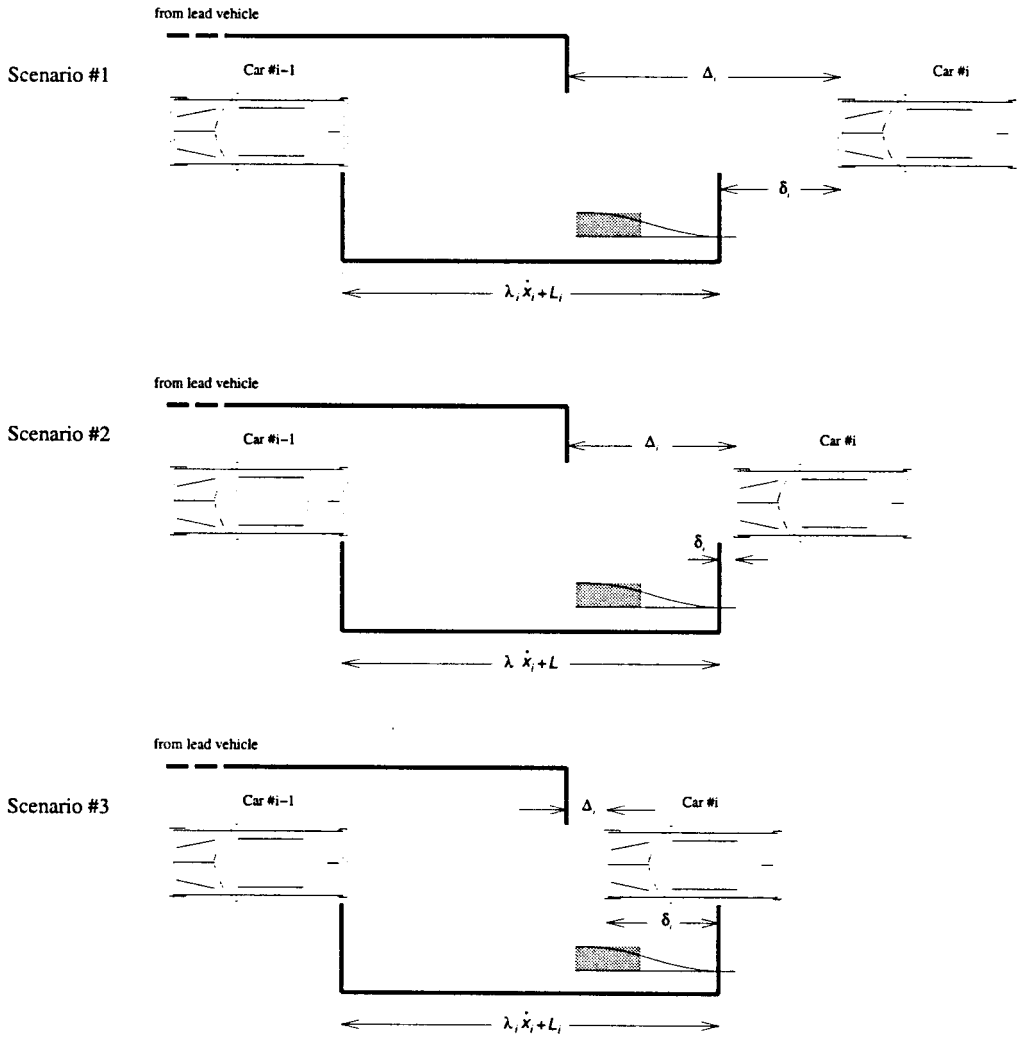

Fig. 4. An illustration of different driving scenarios.

the global string position may be tracked; on the other hand, $\Pi(\cdot) \in (0, 1]$ implies that the position of the preceding vehicle should be taken into account before tracking the global string position. It should be noted that $\Delta_i - \delta_i$ is a signal which is independent of the current state of the ith vehicle. Fig. 3 shows the general form of $\Pi(\cdot)$ used within the collision-avoidance scheme. The region to the right of $-a$ is where $\Pi(\cdot)$ is small and it thus represents the safe distance operating region. The point $-a$ is the closest that the following vehicle should get to the preceding vehicle since when $\Pi(\cdot) = 1$ the error becomes $e_i = \delta_i - a$.

Fig. 4 demonstrates three different tracking scenarios within an AHS. Scenario #1 shows the case where the ith vehicle is too far behind both the $i-1$st vehicle and its string position. In this case, it is necessary for the ith vehicle to move forward along the string. After moving forward, Scenario #2 may occur at which point the ith vehicle should not move too much more forward, even though its string position relative to the lead vehicle has not yet been reached. If the ith vehicle does continue to move forward, then Scenario #3 may occur in which the ith vehicle is too close to the $i-1$st vehicle and the headway policy is not maintained. Thus there may be times when tracking the string position without consideration of local conditions may result in an unsafe driving environment. Using our formulation, in this case we have $\Delta_i - \delta_i < -a$ and $0 < \Pi(\Delta_i - \delta_i) \leq 1$ so that we use $e_i = \Delta_i + z_i$ and the controller will try to reduce both the cumulative error Δ_i and the intervehicle error, δ_i. Notice that if $\Delta_i - \delta_i < 0$ is large enough, then $\Pi(\Delta_i - \delta_i) = 1$ and we have a very unsafe driving condition. However, in this case $e_i = \delta_i - a$ so that our controller is no longer concerned with reducing Δ_i; it simply focuses on correcting the intervehicle spacing error so that we return to a safe driving condition. Finally, we emphasize that the designer specifies the shape and positioning of the $\Pi(\cdot)$ function; hence the designer specifies the acceptable safety regions.

C. Sliding Mode Control

We seek to drive the error, defined by (33), to zero. The error is now expressed as[3]

$$\ddot{e} = \alpha_1(t) + \hat{\alpha}_1(t) + \beta_1\{\alpha_2(t) + \hat{\alpha}_2(t) + \beta_2 u\} \qquad (35)$$

[3]For notational simplicity, the states and control variables hereafter are assumed to be associated with the ith automobile unless subscripts explicitly state otherwise.

where $\alpha_1(t)$ and $\alpha_2(t)$ are known time-varying signals, $|\hat{\alpha}_1(t)| \leq A_1(t)$ and $|\hat{\alpha}_2(t)| \leq A_2(t)$, $\beta_1 \in [\beta_{\min_1}, \beta_{\max_1}]$ and $\beta_2 \in [\beta_{\min_2}, \beta_{\max_2}]$, and u is the control input. The bounds $A_1(t)$, $A_2(t) \geq 0$, and $\beta_{\min_1}$, $\beta_{\max_1}$, $\beta_{\min_2}$, $\beta_{\max_2} > 0$ may be determined for driving and braking scenarios from the equations given below.

The longitudinal dynamics with a driving input (i.e., $u_b = 0$) fits the form of (35) with

$$\alpha_1(t) = -\frac{2\lambda A_{\rho_x}}{m}\dot{x}\ddot{x} - \frac{\lambda}{mR\tau_b}\hat{h}_b\hat{T}_b + (\ddot{x} - \hat{a}_{i-1}) \tag{36}$$

$$A_1(t) = A_z + F_x(X,t) + D_{x3}(X,t) + E_a + \lambda\frac{h_{b_{\max}} - h_{b_{\min}}}{2mR\tau_b}|\hat{T}_b| + \frac{h_{b_{max}}}{mR\tau_b}[D_b(X,t) + E_b] \tag{37}$$

$$\alpha_2(t) = -\hat{T}_e \tag{38}$$

$$A_2(t) = D_e(X,t) + E_d \tag{39}$$

$$\beta_1(t) = \frac{\lambda}{mRR_g\tau_e}h_d \tag{40}$$

$$\beta_2(t) = \gamma_d \tag{41}$$

where $\hat{T}_b$, $\hat{T}_d$, and $\hat{a}_{i-1}$ are estimates of T_b, T_e, and a_{i-1}, respectively, and $|(d^2/dt^2)(\Delta - \delta_i + z)| \leq A_z$. Similarly, the longitudinal dynamics with a braking input (i.e., $u_d = 0$) is defined by (35) with

$$\alpha_1(t) = -\frac{2\lambda A_{\rho_x}}{m}\dot{x}\ddot{x} - \frac{\lambda}{mRR_g\tau_b}\hat{h}_d\hat{T}_d + (\ddot{x} - \hat{a}_{i-1}) \tag{42}$$

$$A_1(t) = A_z + F_x(X,t) + D_{x3}(X,t) + \frac{E_a}{\lambda} + \lambda\frac{h_{b_{\max}} - h_{b_{\min}}}{2mR\tau_d}|\hat{T}_d|P + \frac{h_{b_{\max}}}{mR\tau_b}[D_d(X,t) + E_d] \tag{43}$$

$$\alpha_2(t) = -\hat{T}_b \tag{44}$$

$$A_2(t) = D_b(X,t) + E_b \tag{45}$$

$$\beta_1(t) = \frac{\lambda h_b}{mR\tau_b} \tag{46}$$

$$\beta_2(t) = \gamma_b. \tag{47}$$

Within the above, we define $\hat{h}_d = (h_{d_{\min}} + h_{d_{\max}})/2$ and $\hat{h}_b = (h_{b_{\min}} + h_{b_{\max}})/2$. The estimation errors E_a, E_d, and E_b will be defined within the next section. Partial derivatives may be used to determine $(d^2/dt^2)(\Delta - \delta_i + z)$, otherwise, this quantity may be estimated and the uncertainty absorbed into A_1.

Consider a surface within the state space which passes through the origin, defining the intervehicular spacing between the ith and $i-1$st vehicles as

$$s = \dot{e} + c_2 e + c_1\int_{t_0}^{t} e\,d\tau = 0. \tag{48}$$

The values of c_1 and c_2 are chosen such that if $s_i = 0$, then $e \to 0$ exponentially. This is equivalent to s_i being Hurwitz in p, where $p := d/dt$ is the differential operator. At this point it becomes clear that it is desirable to stay on the surface defined by $s_i = 0$ so that the state trajectory *slides* along the surface to the point $e = 0$. Hence, the controllers we develop will continually seek to drive the system to the *sliding surface*, $s_i = 0$.

Since the controller outputs may saturate, the error surface is modified slightly to prevent integral windup. The new longitudinal error surface is defined as

$$s = \dot{e} + c_2 e + c_1\int_{t_0}^{t} e^*\,d\tau \tag{49}$$

where e is as defined before, and

$$e^* := \begin{cases} e, & \text{if the control inputs are not saturated} \\ 0, & \text{otherwise.} \end{cases} \tag{50}$$

Defining the integral term this way prevents it from increasing, or decreasing, during actuator saturation to help minimize overshoot once the actuators are no longer saturated. By doing this, the sliding surface s_i changes depending upon the state of the ith automobile. Though traditionally an integral term is not needed to ensure exact tracking using sliding-mode control theory, we incorporate the integral term here since we later smooth the control action. The integral term thus provides the tracking advantages associated with proportional-integral-derivative (PID) control action within a boundary layer (i.e., a small region around the surface $s = 0$), while outside the boundary layer we take advantage of the fast convergence properties associated with variable structure control [14]. The use of integral feedback may be eliminated by setting $c_1 = 0$ (it may be desirable to eliminate integral feedback if the faults or time-varying disturbances are fast with respect to the closed-loop plant dynamics).

Using (49) for the ith automobile

$$s = [c_1 \quad c_2 \quad 1]\begin{bmatrix}\int_{t_0}^{t} e^*\,d\tau \\ e \\ \dot{e}\end{bmatrix}. \tag{51}$$

$$\frac{1}{2}\frac{d}{dt}s^2 = s\dot{s} = s\left(C\begin{bmatrix}e^* \\ \dot{e}\end{bmatrix} + \ddot{e}\right) \tag{52}$$

where $C := [c_1 \; c_2]$. The existence of the first and second partials of $\Pi(\cdot)$ is required for the application of Lyapunov stability proofs (i.e., $\dot{e}$ must be continuously differentiable), thus it is assumed that $\Pi(\cdot)$ is defined to be smooth. Substituting (35) into (52) results in

$$s\dot{s} = s\left\{C\begin{bmatrix}e^* \\ \dot{e}\end{bmatrix} + \alpha_1(t) + \hat{\alpha}_1(t) + \beta_1[\alpha_2(t) + \hat{\alpha}_2(t) + \beta_2 u]\right\}. \tag{53}$$

A controller will be defined such that s^2 in nonincreasing ($s\dot{s} \leq 0$).

D. State Estimation

Notice that the longitudinal error dynamics are dependent upon the engine and brake torques, T_e and T_b, respectively, and upon the acceleration of the $i-1$st vehicle, $\ddot{x}_{i-1}$. To reduce the number of needed sensors, we now define estimators for the engine torque $\hat{T}_e$, brake torque $\hat{T}_b$, and the acceleration of the $i-1$st vehicle $\hat{a}_{i-1}$. The input signals to the engine and

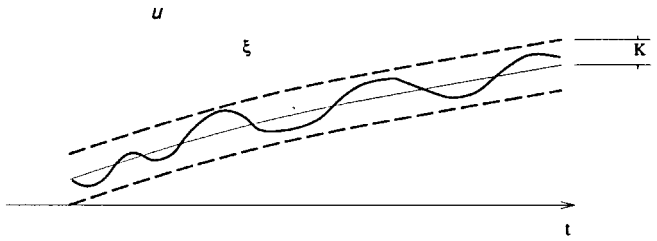

Fig. 5. A typical input to the automobile engine or brake systems.

brakes, u_d and u_b, may be expressed as

$$u_d = \xi_d(t) + \kappa_d(t) \tag{54}$$

$$u_b = \xi_b(t) + \kappa_b(t) \tag{55}$$

where $|\dot{\xi}_d|_\infty \leq \Xi_d$, $|\dot{\xi}_b|_\infty \leq \Xi_b$, $|\kappa_d(t)|_\infty \leq K_d$, and $|\kappa_b(t)|_\infty \leq K_b$. This type of input signal is illustrated in Fig. 5. Consider the following open-loop estimates for the driving and braking torques:

$$\tau_e \frac{d}{dt}\hat{T}_e = u_d - \hat{T}_e \tag{56}$$

$$\tau_b \frac{d}{dt}\hat{T}_b = u_b - \hat{T}_b. \tag{57}$$

The error between the actual and estimated values for the driving and braking torques are given by $e_d := T_e - \hat{T}_e$ and $e_b := T_b - \hat{T}_b$, respectively. The derivative of the error may be found using (15), (19), and (25), with the above torque estimate definitions, (56) and (57), as follows:

$$\tau_e \dot{e}_d = [(\gamma_d - 1)u_d + d_e - e_d] \tag{58}$$

$$\tau_b \dot{e}_b = [(\gamma_b - 1)u_b + d_b - e_b]. \tag{59}$$

(Notice that the error dynamics of the estimates are dependent upon multiplicative uncertainty created by faults in the engine γ_d and brakes γ_b, since the estimates are defined assuming fault-free subsystems.) The following bounds are thus obtained for the torque estimates:

$$\begin{aligned} |e_d| &\leq |(\gamma_d - 1)(\tau_e \Xi_d + K_d) + d_e| \\ &\leq E_d := \max(|\gamma_{d_{\min}} - 1|, \\ &\qquad |\gamma_{d_{\max}} - 1|)|\tau_e \Xi_d + K_d| + D_e(X, t) \end{aligned} \tag{60}$$

$$\begin{aligned} |e_b| &\leq |(\gamma_b - 1)(\tau_e \Xi_b + K_b) + d_b| \\ &\leq E_b := \max(|\gamma_{b_{\min}} - 1|, \\ &\qquad |\gamma_{b_{\max}} - 1|)|\tau_b \Xi_b + K_b| + D_b(X, t). \end{aligned} \tag{61}$$

The estimate of $\ddot{x}_{i-1}$ is defined as $\hat{a}_{i-1} := v_{i-1}/\tau_a - z_a$, where $\tau_a > 0$ is the estimator time constant which may be arbitrarily set, and $\tau_a \dot{z}_a = -z_a + v/\tau_a$. With this estimate, the bound on the error between the actual and estimated accelerations are given as $\|e_a\|_\infty \leq E_a := \tau_a \|x_{i-1}^{(3)}\|_\infty$, where $e_a := \ddot{x}_{i-1} - \hat{a}_{i-1}$. Each estimate bound assumes that the estimator transients have died out. This requires that the estimators be activated for a short time prior to the activation of the longitudinal controller. Since τ_e and τ_b are small, and τ_a may be arbitrarily small, this poses a small problem. For example, the estimators for the engine and brake torques may be activated along the entrance ramp, prior to entering the AHS, and the estimator for $\ddot{x}_{i-1}$ may be activated once communication between the vehicles has been established, prior to the activation of controllers.

E. Control Laws

Since brake and drive torques oppose one another, it is assumed that either a driving input, a brake input, or neither shall be applied at any given time. This excludes the undesirable (and inefficient) simultaneous application of both throttle and brake inputs. Consider the following control laws:

$$u = u_1 + u_2 \tag{62}$$

where

$$u_1 = \frac{1}{\hat{b}_1}\left\{-C\begin{bmatrix} e^* \\ \dot{e} \end{bmatrix} - \alpha_1(t) - k_1 \mathrm{sgn}(s)\right\} \tag{63}$$

$$u_2 = \frac{1}{\hat{b}_2}\left[-\alpha_2(t) - k_2 \mathrm{sgn}(s)\right] \tag{64}$$

with

$$\hat{b}_1 = \sqrt{\beta_{\min_1}\beta_{\max_1}\beta_{\min_2}\beta_{\max_2}} \tag{65}$$

$$\hat{b}_2 = \sqrt{\beta_{\min_2}\beta_{\max_2}} \tag{66}$$

$$k_1 = \hat{\beta}_1(A_1 + \kappa + \eta s) + (\hat{\beta}_1)\left|C\begin{bmatrix} e^* \\ \dot{e} \end{bmatrix} + \alpha_1\right| \tag{67}$$

$$k_2 = \hat{\beta}_2 A_2 + (\hat{\beta}_2 - 1)|\alpha_2| \tag{68}$$

$$\hat{\beta}_1 = \sqrt{\frac{\beta_{\max_1}\beta_{\max_2}}{\beta_{\min_1}\beta_{\min_2}}} \tag{69}$$

$$\hat{\beta}_2 = \sqrt{\frac{\beta_{\max_2}}{\beta_{\min_2}}} \tag{70}$$

and where κ, $\eta > 0$ are design parameters used to set the error convergence rate. Here, we define

$$\mathrm{sgn}(s) = \begin{cases} 1, & s > 0 \\ -1, & s < 0. \end{cases} \tag{71}$$

We first prove that the above control law ensures exponential stability for systems defined by (35), and then show how to apply this to coordinate control between the brakes and throttle.

Directly substituting (62) into (53) we obtain

$$\begin{aligned} s\dot{s} = s\Bigg\{&\left(C\begin{bmatrix} e^* \\ \dot{e} \end{bmatrix} + \alpha_1(t)\right)\left(1 - \frac{\beta_1\beta_2}{\hat{b}_1}\right) \\ &+ \hat{\alpha}_1(t) - \frac{\beta_1\beta_2}{\hat{b}_1} k_1 \mathrm{sgn}(s) \\ &+ \beta_1\left[\alpha_2(t)\left(1 - \frac{\beta_2}{\hat{b}_2}\right) + \hat{\alpha}_2(t) - \frac{\beta_2}{\hat{b}_2} k_2 \mathrm{sgn}(s)\right]\Bigg\} \\ &- \frac{\eta\beta_1\beta_2}{\beta_{\min_1}\beta_{\min_2}} s^2. \end{aligned} \tag{72}$$

Since

$$\frac{\beta_1\beta_2}{\hat{b}_1}(\hat{\beta}_1 - 1) \geq \left|1 - \frac{\beta_1\beta_2}{\hat{b}_1}\right|$$

TABLE I
CONTROL INPUTS FOR DIFFERENT OPERATING REGIONS

	$\bar{u}_d > 0,\ \bar{u}_b > 0$	$\bar{u}_d > 0,\ \bar{u}_b \leq 0$	$\bar{u}_d \leq 0,\ \bar{u}_b > 0$	$\bar{u}_d \leq 0, \bar{u}_b \leq 0$
$u_d =$	$\bar{u}_d$	0	0	0
$u_b =$	0	0	0	$\bar{u}_b$

we use the definition of k_1 so that the first part of (72) is

$$s\left\{\left(C\begin{bmatrix}e^*\\ \dot{e}\end{bmatrix}+\alpha_1(t)\right)\left(1-\frac{\beta_1\beta_2}{\hat{b}_1}\right)-\left|C\begin{bmatrix}e^*\\ \dot{e}\end{bmatrix}\right| +\alpha_1(t)\left|\frac{\beta_1\beta_2(\hat{\beta}_1-1)}{\hat{b}_1}\mathrm{sgn}(s)\right\}\leq 0 \quad (73)$$

and since

$$\frac{\beta_2}{\hat{b}_2}(\hat{\beta}_2-1)\geq\left|1-\frac{\beta_2}{\hat{b}_2}\right|$$

we may use k_2 so that

$$s\beta_1\left\{\alpha_2(t)\left(1-\frac{\beta_2}{\hat{b}_2}\right)-|\alpha_1(t)|\,\frac{\beta_2(\hat{\beta}_2-1)}{\hat{b}_2}\mathrm{sgn}(s)\right\}\leq 0. \quad (74)$$

Also note that

$$s\left\{\hat{\alpha}_1(t)-\frac{\beta_1\beta_2\hat{\beta}_1}{\hat{b}_1}A_1\mathrm{sgn}(s)\right\}\leq 0$$

and

$$s\beta_1\left\{\hat{\alpha}_2-\frac{\beta_2\hat{\beta}_2}{\hat{b}_2}A_2\mathrm{sgn}(s)\right\}\leq 0$$

so that

$$s\dot{s}\leq-\kappa|s|-\eta s^2. \quad (75)$$

This establishes at least "exponential convergence" [15] to the sliding surface as desired since $s\dot{s}\leq-\eta s^2$ and also establishes finite time convergence since $s\dot{s}\leq-\kappa|s|$.

The longitudinal dynamics contain both drive and brake subsystems, however, so we now need to determine how to coordinate the control action so that exponential convergence is still guaranteed. If the drive input is able to take on both positive and negative values, and the brake input was set to $u_b=0$, then defining u_d according to (62)–(70) would force $s\to 0$ as desired. Similarly, if the brake input could take on both positive and negative values, while maintaining $u_d=0$, then $s\to 0$. Define the intermediate control term $\overline{u}_d=u$, where u is defined by (62), with the dynamics defined by the driving dynamics and $u_b=0$. Also define $\overline{u}_b=u$, where u is again defined by (62), with the dynamics defined by the braking dynamics and $u_d=0$. Since the controller gain for both the driving and braking dynamics is positive, we may now define the final control terms u_d and u_b as in Table I.

To see that $s\dot{s}\leq-\eta s^2$ is maintained at all times, we will consider each column of Table I. In the first column, u_d is a positive driving torque, thus u_b may be set to zero, ensuring convergence to the sliding surface, as shown by (75). The second and third columns are obtained since if both a negative and a positive torque control input ensure convergence to the sliding surface, then an input of zero also ensures convergence to $s=0$, since the input gains on u_d and u_b are positive at all times. The fourth column also ensures convergence to the sliding surface since u_b is a negative braking torque and we may set $u_d=0$. Convergence to the sliding surface is thus ensured at all time assuming that the actuators do not saturate. Columns 2 and 3 of Table I introduce a "dead zone" in the control algorithm in which the automobile is allowed to coast without the application of throttle or brakes.

The throttle angle may be found by inverting (16)–(18), i.e., by inverting the engine torque map. Thus

$$\alpha=\mathrm{TC}^{-1}\left[\max\left(1,\ \frac{\omega_e u_d}{\mathrm{MAX}\cdot T_{\max}\cdot\mathrm{AFI}}\right)\right] \quad (76)$$

and

$$\mathrm{TC}^{-1}(\beta)=\frac{\frac{180}{\pi}\cos^{-1}(1-\beta)+1.0600}{1.4459}. \quad (77)$$

Since TC may take on a maximum value of 1.0, the maximum engine torque is

$$T_{d_{\max}}=\frac{T_{\max}\,\mathrm{MAX}\cdot\mathrm{AFI}}{\omega_e}. \quad (78)$$

The above control laws thus establish local exponential stability of the system [15].

We have thus far developed a sliding-mode controller capable of compensating for a class of faults within an AHS. This ensures that the controller will maintain proper vehicle following, even in the presence of faults, up to the limits of the automobile and controllers. Once the actuators saturate, however, stability is no longer guaranteed. This simply implies that the controllers cannot provide a performance level that an automobile is not capable of delivering. For example, if an automobile must come to a complete stop from 60 mi/h in 10 m on an icy road, once the brakes saturate, we are no longer guaranteed convergence to $s_{lon}=0$. If the actuators do not saturate and we consider vehicles without communication capabilities, then stability of the string is established since the intervehicle spacing error for each vehicle decreases exponentially as shown in [10].

Sliding-mode controllers can induce "chattering" due to small unmodeled time delays within the automobile. Here, the control laws are "smoothed" by replacing each $\mathrm{sgn}(s)$ with $\mathrm{sat}(s/\gamma)$, $\gamma>0$ where

$$\mathrm{sat}(x)=\begin{cases}1, & \text{if } 1<x\\ x, & \text{if } -1\leq x\leq 1\\ -1, & \text{if } x<-1.\end{cases} \quad (79)$$

TABLE II
AUTOMOBILE PARAMETERS USED FOR SIMULATION

Vehicle Parameters			
m	$1300Kg$	a	$1.26m$
b	$1.6m$	c	$0.78m$
d	$0.78m$	T_{aux}	$0Nm$
MAX	$0.1843kg/s$	R_d	1.2
R_g	0.351	I_z	$1969kg \cdot m^2$
τ_b	$0.072s$	τ_e	$0.1s$
$T_{d_{max}}$	1500	$T_{b_{max}}$	1500
A_{ρ_x}	0.4298		

Smoothing the control action in this way will ensure that s will converge to a γ-neighborhood of $s = 0$. Since the manifold is stable, we are guaranteed that e will converge to a neighborhood which is proportional to γ. It should be noted that a similar lateral controller was developed in [16].

V. SIMULATION STUDIES

A series of simulations were conducted to test the performance of the above proposed controller. The automobile model defined within Section II was used for controller development, while within this section the complex automobile model described in [11], except for the powertrain, was used for the simulations. The powertrain defined by (15)–(18) was used since the powertrain within [11] contains pure time delays. The simulation model includes suspension dynamics, time lag in the brakes, and powertrain, wheel dynamics, including slip curves for road surface selection, and pitch, roll, and yaw dynamics in addition to road profile selection so that hills and road curves may be chosen to represent a wide range of highways. The automobile parameters that we use for all the vehicles in the automated lane are summarized in Table II (it should be noted that additional parameters are used within the simulation model [11], though are not completely defined here due to space limitations).

The ith vehicle's controller requires the measurement of the variables shown in Table III, plus any additional variables used for the engine torque map inversion (using the inverse torque map defined by (76), the measurement of ω_e would also be required). The variables $\sum_{j=l}^{i-1} \Phi_j$ and $\sum_{j=l}^{i-1} \dot{\Phi}_j$ are measured if communications are available, where the lth vehicle is the first vehicle down the string toward the lead vehicle which does not have communication capabilities. If the $i-1$st vehicle does not have communication capabilities, then we simply set $\Delta_i = \delta_i$. The safety function is defined as

$$\Pi(x) = \begin{cases} 0, & \text{if } x > 0 \\ \sin^2\left(\dfrac{-\pi x}{2b}\right), & \text{if } -b \le x \le 0 \\ 1, & \text{if } x < -b \end{cases} \tag{80}$$

where we chose $b = 4$ and $a = 2$ (in (34)).

The controller parameters are shown in Table IV. The choice of $\lambda = 0.3$ and $L = 4$ will provide a considerable increase in vehicle flow rate over what is achieved by humans. The sliding surfaces were chosen such that the corresponding poles of the error surface would lie along the negative real axis at -1.5 and -0.1. The value of γ_x was chosen to allow s_{lon} to remain in a moderate size boundary layer, while maintaining small tracking errors. For the simulations, the bounds on the function errors for the longitudinal dynamics were taken as $A_1 = 0.2$ and $A_2 = 50$. This corresponds to the tolerated uncertainty in longitudinal acceleration to be 0.2 m/s^2 and the tolerated uncertainty in either engine or brake torque to be 50 N $\cdot$ m.

TABLE III
AUTOMOBILE VARIABLES REQUIRED FOR CONTROL WITHOUT VEHICLE COMMUNICATIONS

Measured Variables without communications	
$x_i - x_{i-1}$	$\dot{x}_i - \dot{x}_{i-1}$
$\dot{x}_i$	$\ddot{x}_i$

TABLE IV
CONTROLLER PARAMETERS USED WITHIN THE SIMULATION STUDIES

Controller Parameters			
λ	0.3	L	4
η_x	1.0	γ_x	0.05
c_{x1}	0.15	c_{x2}	1.6
$h_{d_{min}}$	0.8	$h_{d_{max}}$	1.0
$h_{b_{min}}$	0.8	$h_{d_{max}}$	1.0
$\gamma_{d_{min}}$	0.9	$\gamma_{d_{max}}$	1.0
$\gamma_{b_{min}}$	0.9	$\gamma_{b_{max}}$	1.0

A. Without Faults

An initial study using a five-vehicle string, in which no vehicle experienced a fault, was run to demonstrate the nominal performance of the longitudinal control scheme. The automobiles are numbered such that the lead vehicle is car #0 with the last following automobile numbered as car #4. For this study, the plots are labeled as car #0 (– · –), car #1 (– – –), car #2 (— —), car #3 (· · · ·), and car #4 (–.–). The case where communication capabilities are not present in any of the five vehicles is considered first. Fig. 6 shows the velocity profiles of the lead vehicle, and four following vehicles. The intervehicle spacing errors, δ_i, $i = 1, \cdots, 4$, are shown in Fig. 7. Although high control energy is typically associated with sliding-mode control, Fig. 8 shows that the control inputs for car #1 are fairly smooth and that there is no rapid changing between the throttle and brakes (control inputs for the other vehicles behave similarly).

A second simulation was conducted to show how the use of intervehicle communications changes the behavior of the vehicles. Here each vehicle within the string is assumed to have communication capabilities. The velocity profiles for the vehicles are shown in Fig. 9 and appear very similar to the no communication case of Fig. 6. The intervehicle spacing errors shown in Fig. 10, however, are much different than those in Fig. 7. With communications, each vehicle within the string is following its associated position with respect to the lead vehicle assuming that each preceding vehicle is achieving

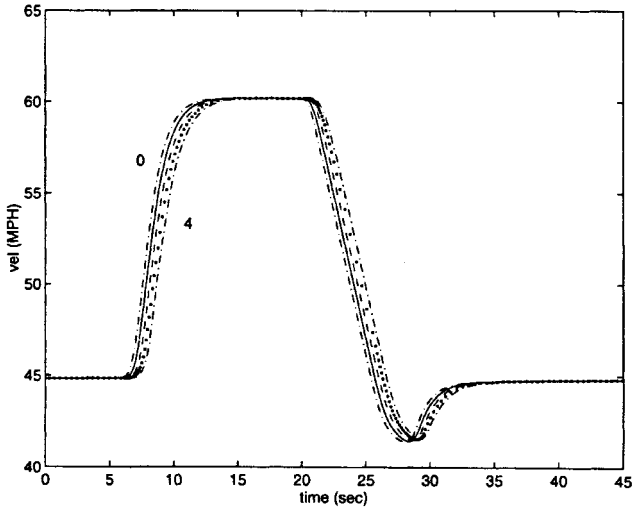

Fig. 6. Velocity profiles (in miles per hour) for the five-vehicle string with no faults and no communications.

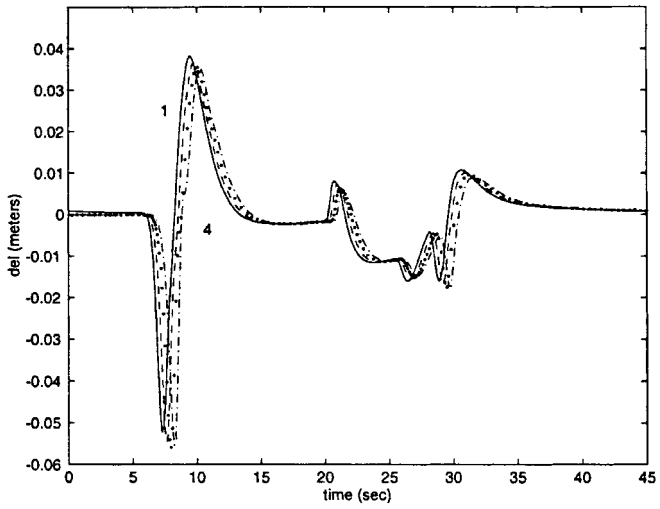

Fig. 7. Intervehicle spacing errors, δ_i, $i = 1, \cdots, 4$, for the five following vehicles with no faults and no communications.

perfect tracking. The unmodeled vehicle dynamics (such as the wheel dynamics) and the smoothing of the control law keep the longitudinal controller from achieving perfect tracking. Since each vehicle is tracking the lead vehicle of the string and each vehicle is subject to the same type of uncertainties, the intervehicle spacing errors for car #2 and higher will be small.[4] To eliminate the tracking errors caused by the filter transients, one could either specify the initial conditions of the filters so that there is no initial tracking error or simply allow the stable filters to run for a few seconds before starting the control algorithms. A similar effect from filter transients is also seen in several of the remaining simulations.

A study was also conducted to test the performance of an AHS with vehicles which do not have communication capabilities and vehicles which do have communication capabilities.

[4]It is important to note that the transient behavior of the filters used to define Δ_i cause an initial tracking error for cars #2, #3, and #4 as seen within Fig. 10.

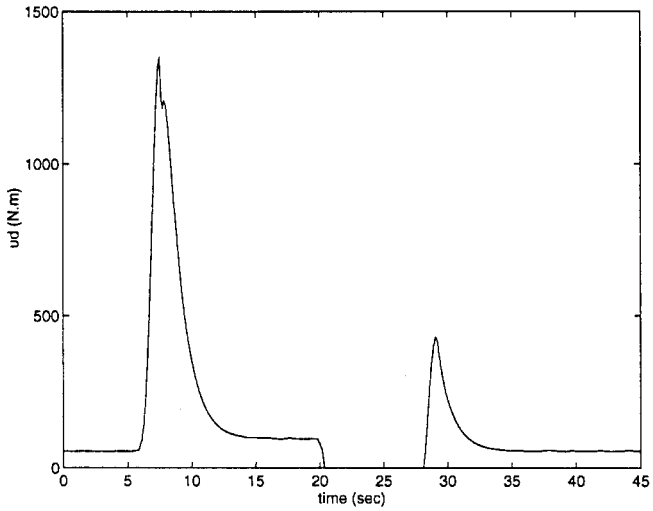

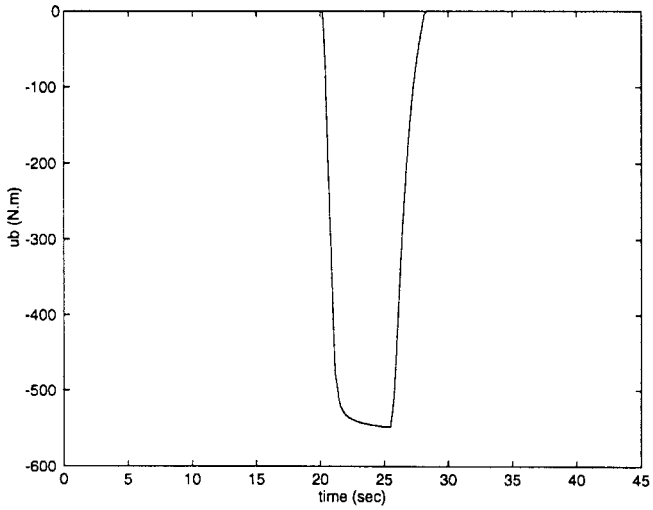

Fig. 8. Engine input u_d and brake input u_b for car #1 with no faults.

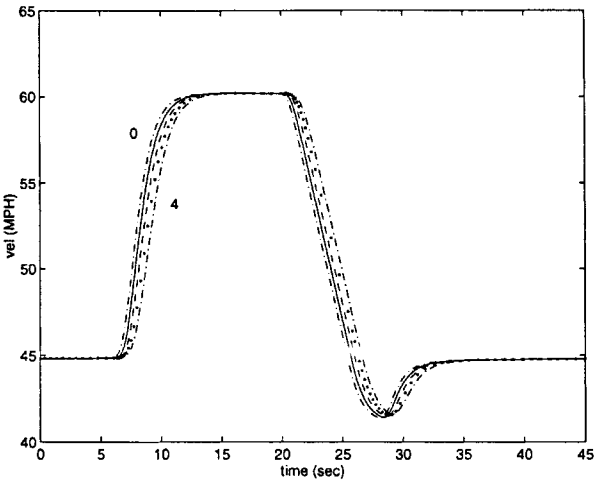

Fig. 9. Velocity profiles (in miles per hour) for the five-vehicle string with communications and no faults.

Here the first three vehicles are able to communicate, while the last two do not have communication capabilities. The velocity profiles for the string are shown in Fig. 11, while

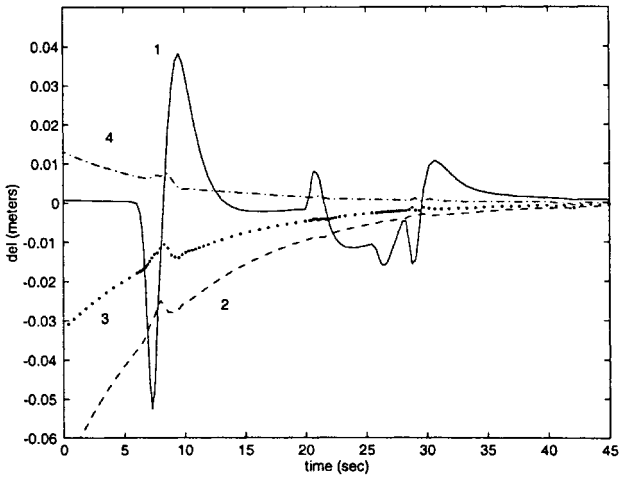

Fig. 10. Intervehicle spacing errors δ_i, $i = 1, \cdots, 4$, for the five following vehicles with communications and no faults.

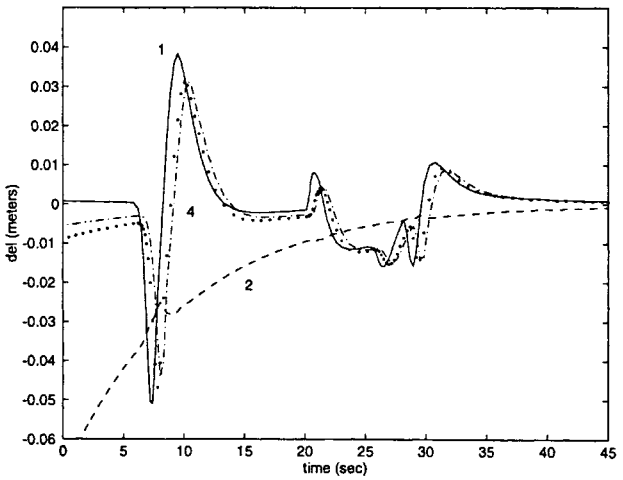

Fig. 12. Intervehicle spacing errors δ_i, $i = 1, \cdots, 4$, for the five following vehicles with hybrid communications and no faults.

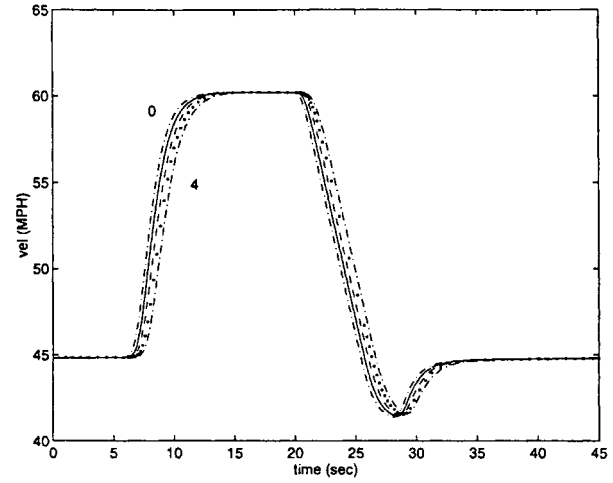

Fig. 11. Velocity profiles (in miles per hour) for the five-vehicle string with hybrid communications and no faults.

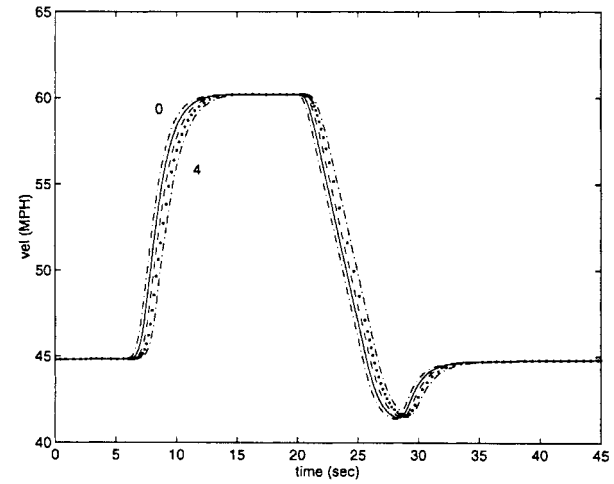

Fig. 13. Velocity profiles for the string with no communications with a fault-induced engine torque in car #1.

the intervehicle spacing errors are shown in Fig. 12. The vehicles which do not communicate have the same type of spacing profiles as found in Fig. 7, while the vehicles which do communicate have spacing profiles similar to Fig. 10.

B. Induced Torque Fault

Assume that during an acceleration and deceleration maneuver, the first following vehicle experiences a sinusoidally varying torque applied to the driveshaft due to a fault with magnitude 40 N · m and frequency 1 rad/s. This may be caused by a mechanical failure in the drivetrain (e.g., friction due to uneven wear of components) or a load torque from another component that is powered by the engine. The velocity profiles of the five automobiles with no communication capabilities are shown in Fig. 13 with the tracking errors shown in Fig. 14. A slight oscillation is seen within the tracking error δ_1, though it is reduced along the string because of the low-pass characteristics of the headway policy.

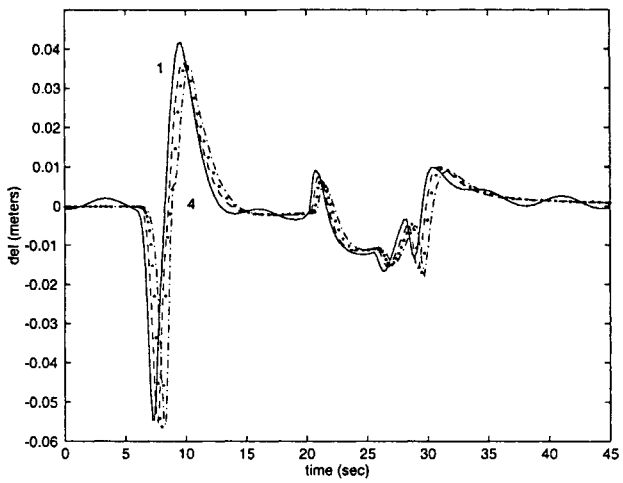

Fig. 14. Tracking errors δ_i for the string with no communications with a fault-induced engine torque in car #1.

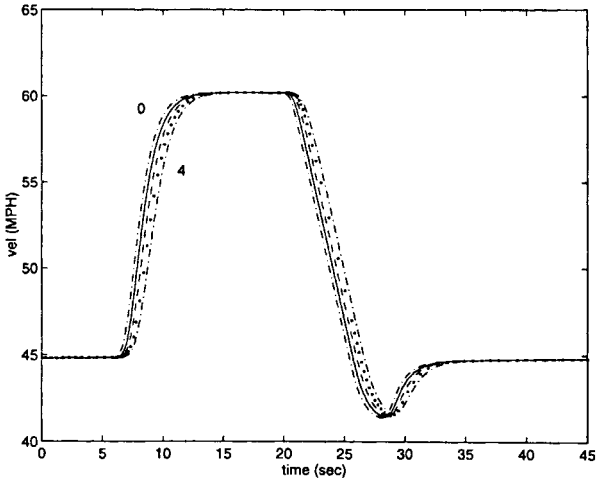

Fig. 15. Velocity profiles for the string with communications with a fault-induced engine torque in car #1.

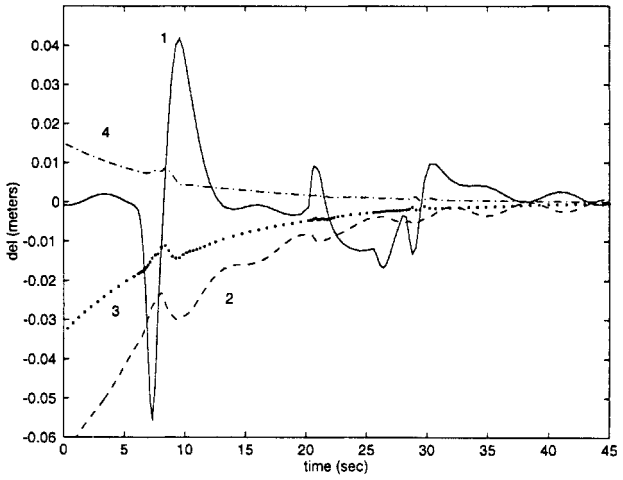

Fig. 16. Tracking errors δ_i for the string with communications with a fault-induced engine torque in car #1.

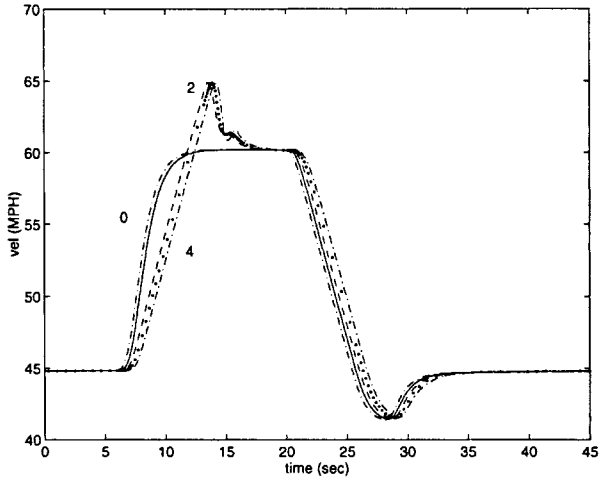

Fig. 17. Velocity profiles for the string without communications with an engine saturation fault in car #2.

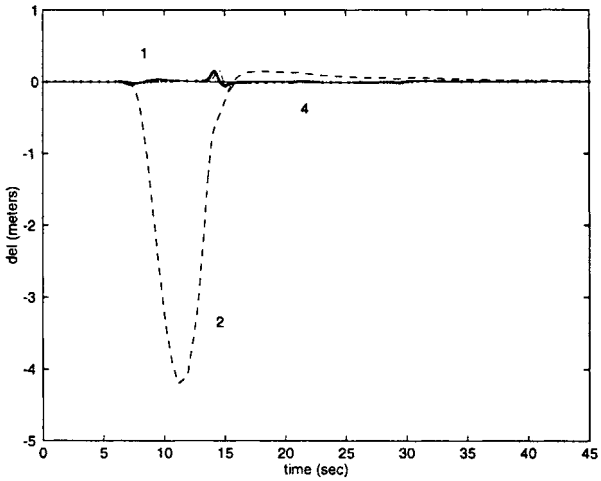

Fig. 18. Tracking errors δ_i for the string without communications with an engine saturation fault in car #2.

Next, the velocity profiles for the case where communication capabilities are present for each vehicle is shown in Fig. 15. The intervehicle spacing errors are shown in Fig. 16. If communications are used then the oscillatory motion caused by the fault is not felt down the string. This is an important consideration for ride comfort. Without communications, if the longitudinal motion for a vehicle at the beginning of the string causes an uncomfortable ride, each following vehicle may experience this same type of ride. The oscillatory characteristic of δ_2 is caused since car #2 is tracking the lead vehicle, which is not oscillating, while the intervehicle spacing error measurement is taken with respect to car #1. Thus car #2 is not actually experiencing any oscillatory effects, rather the spacing reference is oscillating.

C. Faulty Throttle

Within this simulation, it is assumed that the throttle of car #2 is faulty so that the engine input saturates with $T_{d_{\max}} = 700$. The vehicle with the faulty throttle is no longer able to accelerate quickly enough to keep up with the preceding vehicle during the acceleration maneuver. Once again, the case where no communication capabilities are assumed is considered first. The velocity profiles of the five automobiles are shown in Fig. 17 while the tracking errors are shown in Fig. 18. The second vehicle now has to accelerate past the top speed of the lead vehicle so that it catches up to car #1. Since cars #3 and #4 are just following the corresponding preceding vehicles, they also overshoot the velocity of the lead vehicle. Here, only car #2 experiences a large intervehicle spacing error. The engine u_d and brake, u_b inputs are shown in Fig. 19.

Next, vehicle communications are considered. The velocity profiles are shown in Fig. 20 with the intervehicle spacing shown in Fig. 21. Here the intervehicle spacing errors for cars #2, #3, and #4 increase while car #2 attempts to catch up to the preceding vehicles. This is due to the fact that vehicles with communication capabilities consider their string position until they become too close to the preceding vehicle. The driving and braking inputs for car #2 are shown in Fig. 22. If the string

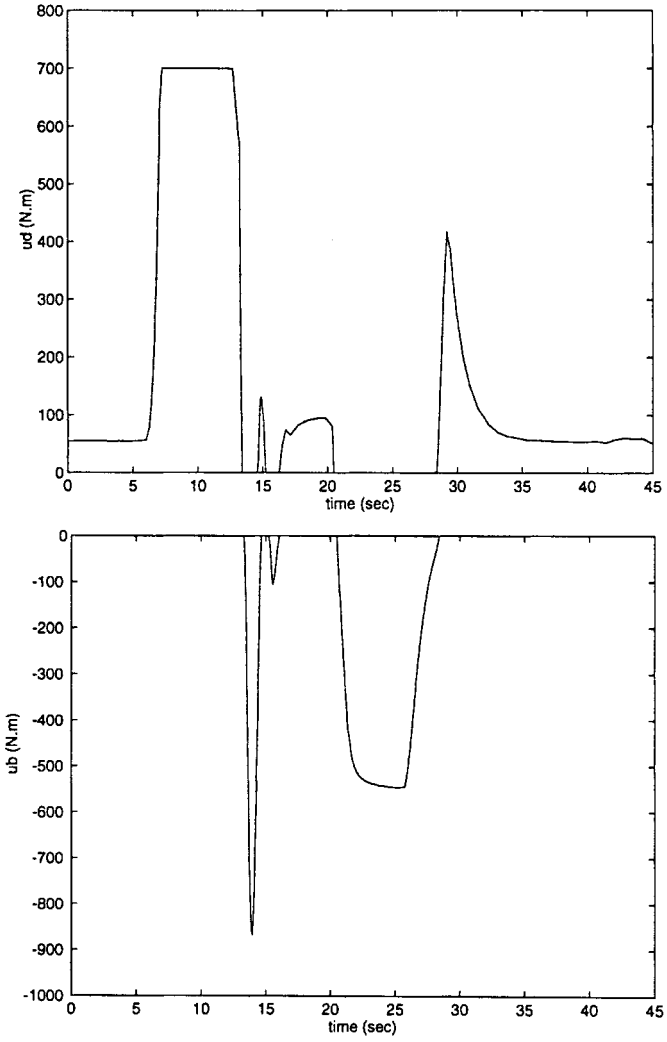

Fig. 19. Engine input u_d and brake input u_b for car #2 with an engine saturation fault without communications.

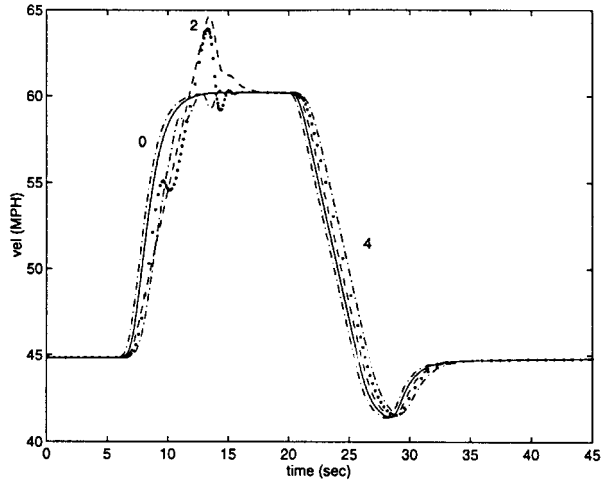

Fig. 20. Velocity profiles for the string with communications with an engine saturation fault in car #2.

is long enough, vehicles at the end of the string may not even notice the effects of car #2 since the spacing deviations would be absorbed by preceding vehicles.

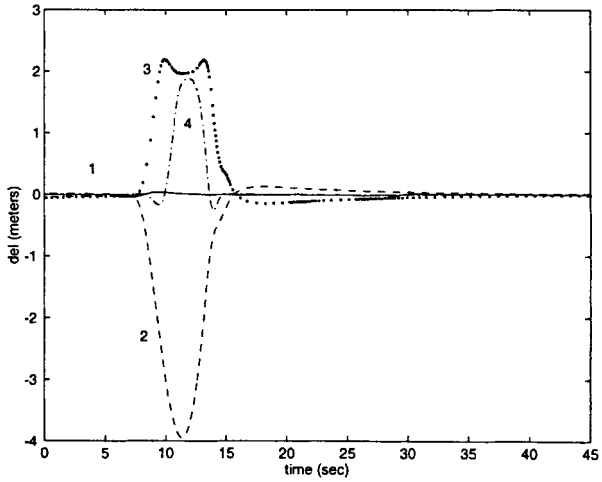

Fig. 21. Tracking errors δ_i for the string with communications with an engine saturation fault in car #2.

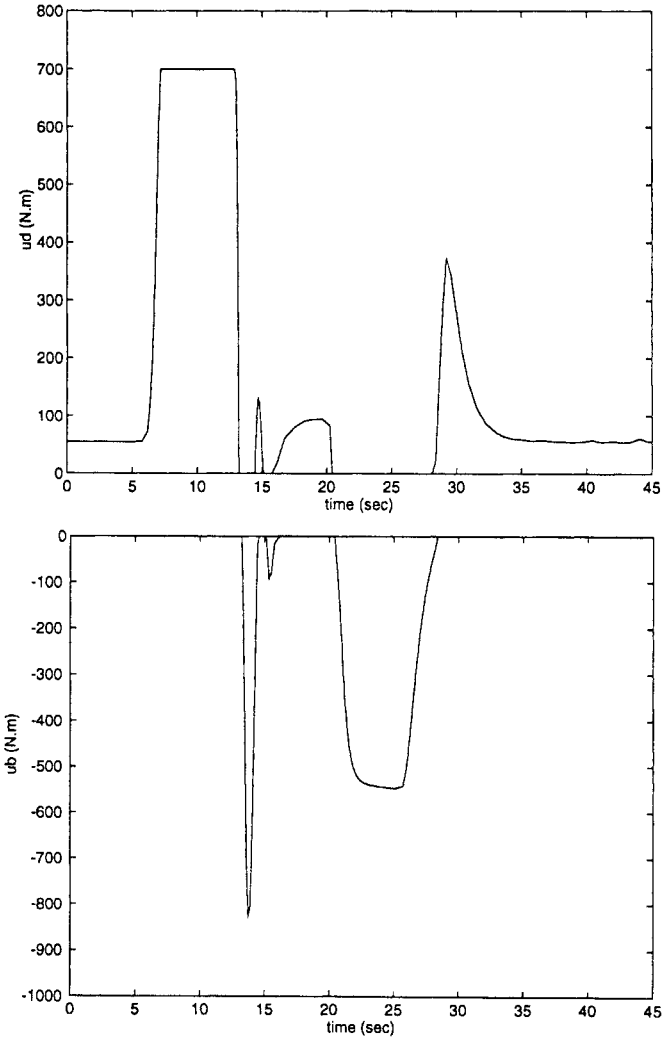

Fig. 22. Engine input, u_d, and brake input, u_b, for car #2 with an engine saturation fault with communications.

VI. Concluding Remarks

Within this paper, a simplified model of an automobile was developed for fault-tolerant controller design. A fault-tolerant longitudinal controller was developed using a sliding-mode

control technique and stability was shown. Simulation studies were performed to demonstrate the performance of the fault-tolerant controllers in the presence of simple automotive and AHS failures. This study has demonstrated that the use of fault-tolerant controller design may provide a high level of safety without sacrificing performance. In future work, there is a need to expand the class of faults which may be tolerated and to evaluate the proposed control strategy in an experimental testbed.

REFERENCES

[1] J. G. Bender, "An overview of systems studies of automated highway systems," *IEEE Trans. Veh. Technol.*, vol. 40, pp. 82–99, Feb. 1991.

[2] P. Varaiya, "Smart cars on smart roads: Problems of control," *IEEE Trans. Automat. Contr.*, vol. 38, pp. 195–207, Feb. 1993.

[3] R. E. Fenton and R. J. Mayhan, "Automated highway studies at The Ohio State University—An overview," *IEEE Trans. Veh. Technol.*, vol. 40, pp. 100–113, Feb. 1991.

[4] S. E. Shladover, C. A. Desoer, J. K. Hedrick, M. Tomizuka, J. Walrand, W.-B. Zhang, D. H. McMahon, H. Peng, S. Sheikholeslam, and N. McKeown, "Automatic vehicle control developments in the PATH program," *IEEE Trans. Veh. Technol.*, vol. 40, pp. 114–130, Feb. 1991.

[5] S. Sheikholeslam and C. A. Desoer, "A system level study of the longitudinal control of a platoon of vehicles," *ASME J. Dyn. Syst. Meas. Contr.*, vol. 114, pp. 286–292, June 1992.

[6] ———, "Longitudinal control of a platoon of vehicles with no communication of lead vehicle information: A system level study," *IEEE Trans. Veh. Technol.*, vol. 42, pp. 546–554, Nov. 1993.

[7] P. A. Ioannou and C. C. Chien, "Autonomous intelligent cruise control," *IEEE Trans. Veh. Technol.*, vol. 42, pp. 657–672, Nov. 1993.

[8] C. C. Chien, P. Ioannou, and M. L. Lai, "Entrainment and vehicle following controllers design for autonomous intelligent vehicles," in *Proc. 1994 American Control Conf.* (Baltimore, MD, 1994), pp. 6–10.

[9] J. K. Hedrick, D. McMahon, V. Narendran, and D. Swaroop, "Longitudinal vehicle controller design for IVHS systems," in *Proc. 1991 American Control Conf.* (Boston, MA, 1991), pp. 3107–3112.

[10] A. Stotsky, C. C. Chien, and P. Ioannou, "Robust platoon-stable controller design for autonomous intelligent vehicles," in *Proc. 33rd Conf. on Decision and Control* (Lake Buena Vista, FL, Dec. 1994), pp. 2431–2435.

[11] J. T. Spooner and K. M. Passino, "Modeling and simulation of automobile dynamics for IVHS studies," Ohio State Univ., IVHS-OSU Rep. 94-04, Apr. 1994.

[12] D. Cho and J. K. Hedrick, "Automotive powertrain modeling for control," *ASME J. Dyn. Syst. Meas. Contr.*, vol. 111, pp. 568–576, Dec. 1989.

[13] D. Swaroop and J. K. Hedrick, "Direct adaptive longitudinal control of vehicle platoons," in *Proc. 33rd Conf. on Decision and Control* (Lake Buena Vista, FL, Dec. 1994), pp. 684–689.

[14] V. I. Utkin, "Variable structure systems with sliding modes," *IEEE Trans. Automat. Contr.*, vol. 22, pp. 212–222, Apr. 1977.

[15] H. K. Khalil, *Nonlinear Systems.* New York: Macmillan, 1992.

[16] J. T. Spooner and K. M. Passino, "Fault tolerant longitudinal and lateral control for automated highway systems," Ohio State Univ., IVHS-OSU Rep. 95-05, Mar. 1995.

Jeffrey T. Spooner received the B.A. degree in physics from Wittenberg University in 1991 and the B.S. degree in electrical engineering from Ohio State University, Columbus, in 1993. In 1995, he received the M.S. degree in electrical engineering with a specialization in control systems.

Since 1995, he has been with the Control Subsystems Department at Sandia National Laboratories, Albuquerque, NM. His areas of interest include adaptive control, fuzzy systems, neural networks, and modeling.

Kevin M. Passino (S'79–M'90–SM'96) received the M.S. and Ph.D. degrees in electrical engineering from the University of Notre Dame, Notre Dame, IN, in 1989 and the B.S.E.E. degree from Tri-State University, Angola, IN, in 1983.

He has worked in the control systems group at Magnavox Electronic Systems Co., Ft. Wayne, IN, on research in missile control and at McDonnell Aircraft Co., St. Louis, MO, on research in flight control. He spent a year at Notre Dame as a Visiting Assistant Professor and is currently an Associate Professor in the Department of Electrical Engineering at Ohio State University, Columbus. He is co-editor (with P. J. Antsaklis) of the book *An Introduction to Intelligent and Autonomous Control* (Kluwer Academic Press, 1993). His research interests include intelligent and autonomous control techniques, nonlinear analysis of intelligent control systems, failure detection and identification systems, and genetic algorithms for control.

Dr. Passino is a member of the IEEE Control Systems Society Board of Governors. He is an Associate Editor for the IEEE TRANSACTIONS ON AUTOMATIC CONTROL, has served as the Guest Editor for the 1993 *IEEE Control Systems Magazine* Special Issue on Intelligent Control, and was a Guest Editor for a special track of papers on Intelligent Control for the *IEEE Expert Magazine* in 1996. He is on the Editorial Board of the *International Journal for Engineering Application of Artificial Intelligence*. He was the Publicity Co-Chair for the IEEE Conference on Decision and Control in Japan in 1996 and is the Workshops Chair for the 1997 IEEE Conference on Decision and Control. He was a Program Chairman for the 8th IEEE International Symposium on Intelligent Control (1993), served as the Finance Chair for the 9th IEEE International Symposium on Intelligent Control, and is serving as the General Chair for the 11th IEEE International Symposium on Intelligent Control.